# Method to control the coupling function using multilinear feedback

T. Kano* and S. Kinoshita
*Graduate School of Frontier Biosciences, Osaka University, Suita 565-0871, Japan*
(Received 17 August 2008; published 19 November 2008)

Methods to control the dynamics of coupled oscillators have been developed owing to various medical and technological demands. In this study, we develop a method to control coupled oscillators in which the coupling function expressed in a phase model is regulated by the multilinear feedback. The present method has wide applicability because we do not need to measure an individual output from each oscillator, but only measure the sum of the outputs from all the oscillators. Moreover, it allows us to easily control the coupling function up to higher harmonics. The validity of the present method is confirmed through a simulation.

DOI: 10.1103/PhysRevE.78.056210 PACS number(s): 05.45.Xt, 82.40.Bj

## I. INTRODUCTION

The spontaneous synchronization of mutually interacting elements exhibiting regular rhythms is a well-known phenomenon in nature, and has been extensively studied from physical, biological, medical, and technological viewpoints [1–12]. It is well known that this synchronization often plays a functional role in either a plausible [4–8] or unplausible manner [9–12]. For example, the synchronous flashing of male fireflies plays the role of attracting the attention of females [4], whereas the pathological synchronization of neurons in patients of Parkinson's disease or essential tremors causes unplausible involuntary movements [9–12].

It has recently been suggested in a variety of fields that controlling the dynamics of coupled-oscillator systems is essential to attain their desirable functions [5–7,9–15]. For example, the use of electrical stimulation techniques [9–13] has been known to be therapeutic for several neural diseases such as Parkinson's disease, essential tremor, and the dysfunction of central pattern generators (CPGs) which are neural networks that allow us to perform movements such as walking, running, and swimming by their synchronization [8]. These therapies have been developed such that the electrical stimulation desynchronizes or locally synchronizes the pathological activities of neurons effectively [9–13]. Another example is found in the field of technology. Many tasks in robotics require cyclic actions to be coordinated, such as walking, juggling, and factory automation. Hence, devising a method for stabilizing a desired phase relationship of cyclic units will be a challenging problem [5–7].

It is well known that signal transmissions among elements constituting a system with different time delays often play an essential role for its dynamical behavior, such as polychronization in neuronal networks [16]. Quite recently, a method for controlling the dynamics of coupled oscillators through several feedback signals with different time delays, which is based on the phase model [1–3], has been proposed [14,15]. In this method, the Fourier coefficients of the coupling function, which determine the dynamics of the system, are controlled by measuring a certain observable of each oscillator and applying several nonlinear time-delayed feedback signals to the entire system. This method has an advantage that it is applicable regardless of the detailed mechanisms of individual oscillators, and that various dynamics can be obtained accurately, such as slow switching [17] and phase clustering [21]. However, because of the nonlinearity of the feedback signals, an individual output from each oscillator should be measured independently, which is often difficult in actual systems; moreover, the calculation becomes extremely complex when the Fourier coefficients are controlled up to higher harmonics.

In this study, we aim to derive a tractable and practical method to control the behaviors of coupled oscillators by regulating the Fourier coefficients of the coupling function up to higher harmonics, which is applicable even in the case where only the sum of the outputs from all the oscillators can be measured. We will consider a multilinear feedback method in which only the delays and strengths of the feedback signals are regulated. We will show how these parameters are determined, and we will also confirm the validity of this method through a simulation based on Bonhoeffer–van der Pol model.

## II. METHOD TO CONTROL THE COUPLING FUNCTION

We consider globally coupled oscillators described by

$$\dot{\mathbf{x}}_i = \mathbf{F}_i(\mathbf{x}_i) + \frac{\epsilon_c}{N}\sum_{j=1}^{N} \mathbf{P}_c(\mathbf{x}_i(t),\mathbf{x}_j(t)), \tag{1}$$

where $N$ is the number of oscillators and $\mathbf{P}_c(\mathbf{x}_i(t),\mathbf{x}_j(t))$ denotes the coupling between the oscillators. $\epsilon_c$ is a nondimensional parameter expressing the coupling strength, which is assumed to be sufficiently smaller than unity. $\mathbf{F}_i(\mathbf{x}_i)$ denotes a set of functions describing a limit cycle. We assume that the frequencies of the oscillators are slightly different from each other in nature with the magnitude of the difference being characterized by $\epsilon_d$ that is smaller than $\epsilon_c$. Then, $\mathbf{F}_i(\mathbf{x}_i)$ is divided into a part common to all the oscillators and the deviation from it as $\mathbf{F}_i(\mathbf{x}_i)=\mathbf{F}(\mathbf{x}_i)+\epsilon_d\mathbf{f}_i(\mathbf{x}_i)$ [we assume that $\mathbf{F}(\mathbf{x}_i)$, $\mathbf{f}_i(\mathbf{x}_i)$, and $\mathbf{P}_c(\mathbf{x}_i(t),\mathbf{x}_j(t))$ are the functions of $O(1)$]. Equation (1) is generally reduced to a phase model as [1]

$$\dot{\phi}_i = \bar{\omega} + \epsilon_d \mathbf{Z}(\phi_i)\cdot\mathbf{f}_i(\mathbf{x}_0(\phi_i)) + \frac{\epsilon_c}{N}\sum_{j=1}^{N}\mathbf{Z}(\phi_i)\cdot\mathbf{P}_c(\mathbf{x}_0(\phi_i),\mathbf{x}_0(\phi_j)), \tag{2}$$

where $\mathbf{x}_0(\phi)$ denotes a point on the limit cycle at a phase $\phi$

*takesik@fbs.osaka-u.ac.jp

 

and $\bar{\omega}$ denotes the increasing rate of the phase when the inhomogeneity $\epsilon_d \mathbf{f}_i(\mathbf{x}_i)$ and the coupling between oscillators are absent. Here, the limit cycle constitutes a closed orbit and hence $\mathbf{x}_0(\phi)=\mathbf{x}_0(\phi+2\pi)$ is naturally satisfied. $\mathbf{Z}(\phi) \equiv (\mathrm{grad}_{\mathbf{x}}\, \phi)_{\mathbf{x}=\mathbf{x}_0(\phi)}$ is called the phase response function, and it is assumed that $|\mathbf{Z}(\phi)|$ does not take an extremely large value for any $\phi$ such that the contributions of the second and third terms in the right-hand side of Eq. (2) are always sufficiently smaller than $\bar{\omega}$. Then, we find from Eq. (2) that $\phi_i - \bar{\omega}t$ evolves slowly as compared to $\phi_i$, and thus we can approximate that $\phi_i - \bar{\omega}t$ is maintained constant during an oscillation period.

Under this approximation, the second and third terms in the right-hand side of Eq. (2) are phase averaged over an oscillation period as

$$\dot{\phi}_i = \bar{\omega} + \epsilon_d \omega_i + \frac{\epsilon_c}{N} \sum_{j=1}^{N} q_c(\phi_i(t) - \phi_j(t)), \tag{3}$$

where

$$\omega_i = \frac{1}{2\pi} \int_0^{2\pi} d\theta \mathbf{Z}(\phi_i + \theta) \cdot \mathbf{f}_i(\mathbf{x}_0(\phi_i + \theta)) \tag{4}$$

and

$$q_c(\phi_i - \phi_j) = \frac{1}{2\pi} \int_0^{2\pi} d\theta \mathbf{Z}(\phi_i + \theta) \cdot \mathbf{P}_{\mathbf{c}}(\mathbf{x}_0(\phi_i + \theta), \mathbf{x}_0(\phi_j + \theta)). \tag{5}$$

$q_c(\phi_i(t) - \phi_j(t))$ is called the coupling function, whose functional form can be experimentally derived either by specifying the phase response function $\mathbf{Z}(\phi)$ [if the interaction $\mathbf{P}_c(\mathbf{x}_i(t), \mathbf{x}_j(t))$ is already known] [19] or by analyzing the period of one of two-coupled oscillators when they are not completely synchronized [20].

In the following, we aim to find appropriate feedback signals applied to the system described by Eq. (1) so that a purpose-designed coupling function $\tilde{q}(\psi)$, which we determine in advance, is obtained. Namely, we will find feedback signals that make Eq. (3) substantially change into

$$\dot{\phi}_i = \bar{\omega} + \epsilon_d \omega_i + \frac{\epsilon_f}{N} \sum_{j=1}^{N} \tilde{q}(\phi_i(t) - \phi_j(t)), \tag{6}$$

where $\epsilon_f$ is the coupling strength under the feedback, which we also determine in advance. $\epsilon_f$ should be sufficiently small such that the phase description is valid, but also sufficiently large such that the oscillators can be synchronized by the feedback even in the presence of the frequency distribution $\epsilon_d \omega_i$. For convenience, let $q_c(\phi_i(t) - \phi_j(t))$ and $\tilde{q}(\phi_i(t) - \phi_j(t))$ be expanded to Fourier series as $q_c(\phi_i(t) - \phi_j(t)) = \Sigma_k a_k^{(c)} \exp[ik(\phi_i(t) - \phi_j(t))]$ and $\tilde{q}(\phi_i(t) - \phi_j(t)) = \Sigma_{k=-M}^{M} \tilde{a}_k \exp[ik(\phi_i(t) - \phi_j(t))]$, where $a_{-k}^{(c)} = a_k^{(c)*}$ and $\tilde{a}_{-k} = \tilde{a}_k^*$ should be satisfied. Here, since we aim to control the coupled oscillators with a finite number of such harmonics, $M$ is defined as the highest harmonic of $\tilde{q}(\phi_i(t) - \phi_j(t))$, up to which the coupling function will be controlled.

We consider the case where the observable in the system is only one, which is expressed as $P_0(t) \equiv \Sigma_{j=1}^{N} p(\mathbf{x}_j(t))$, where $p(\mathbf{x}_j(t))$ is the output from the $j$th oscillator. Here, $p(\mathbf{x}_j(t))$ is arbitrary; however, it should be a single-valued function of $\mathbf{x}_j(t)$ and contain non-negligible Fourier components at least in the harmonics where $a_k^{(c)}$ or $\tilde{a}_k$ has a moderate value. Let the feedback signal be applied to the system of Eq. (1) using this output as

$$\dot{\mathbf{x}}_i = \mathbf{F}_i(\mathbf{x}_i) + \frac{\epsilon_c}{N} \sum_{j=1}^{N} \mathbf{P}_{\mathbf{c}}(\mathbf{x}_i(t), \mathbf{x}_j(t)) + \frac{\epsilon_f}{N} \sum_{m=1}^{2M+1} \Gamma_m P_0(t - \tau_m)\mathbf{r}, \tag{7}$$

where $\tau_m$ and $\Gamma_m$ are the time delay and strength of the $m$th signal, respectively, whose values will be specified later. The number of feedback signals is set at $2M+1$, which is plausible for determining the values of $\tau_m$ and $\Gamma_m$ [see Eq. (13)]. $\mathbf{r}$ is a unit vector whose dimension is equal to that of $\mathbf{x}_i$, and it can be selected in an arbitrary manner. Note that the feedback signal can be attained only through a term $P_0(t)$ and hence any information on each output $p(\mathbf{x}_j(t))$ is not required. This is an excellent and most characteristic point of the present method.

By reducing Eq. (7) to the phase model and phase averaging over an oscillation period [1], we obtain

$$\dot{\phi}_i = \bar{\omega} + \epsilon_d \omega_i + \frac{\epsilon_c}{N} \sum_{j=1}^{N} q_c(\phi_i(t) - \phi_j(t)) + \frac{\epsilon_f}{N} \sum_{m=1}^{2M+1} \Gamma_m \sum_{j=1}^{N} q_f(\phi_i(t) - \phi_j(t - \tau_m)), \tag{8}$$

where

$$\sum_{j=1}^{N} q_f(\phi_i(t) - \phi_j(t - \tau_m)) = \frac{1}{2\pi} \int_0^{2\pi} d\theta \mathbf{Z}(\phi_i(t) + \theta) \cdot \sum_{j=1}^{N} p(\mathbf{x}_0(\phi_j(t - \tau_m) + \theta))\mathbf{r}. \tag{9}$$

Here, the contributions of the second to fourth terms in the right-hand side of Eq. (8) should be sufficiently smaller than $\bar{\omega}$ so that this phase reduction is valid, because it is assumed in the phase-averaging process that $\phi_i - \bar{\omega}t$ is maintained constant during the oscillation period.

The functional form of $q_f(\phi_i(t) - \phi_j(t))$ can be derived in the actual system either by specifying the function $\mathbf{Z}(\phi) \cdot \mathbf{r}$ [19] or by using the method described in Ref. [20], where the details of the latter method are shown in Appendix. The obtained coupling function is expanded to a Fourier series as $q_f(\psi) = \Sigma_k a_k^{(f)} \exp[ik\psi]$, where $a_{-k}^{(f)} = a_k^{(f)*}$ should be satisfied.

Next, we will find the values of $\tau_m$ and $\Gamma_m$ so that the desired coupling function $\tilde{q}(\phi_i(t) - \phi_j(t))$ is obtained. When $\tau_m$ is comparable to or shorter than the natural oscillation period, we can use the following approximation since $\dot{\phi}_j$ is nearly equal to $\bar{\omega}$ [see Eq. (8)]:

$$\phi_j(t-\tau_m) \approx \phi_j(t) - \bar{\omega}\tau_m. \tag{10}$$

Thus, since Eq. (8) is consistent with Eq. (6), the following relation holds:

$$\tilde{q}(\phi_i(t)-\phi_j(t)) = \frac{\epsilon_c}{\epsilon_f} q_c(\phi_i(t)-\phi_j(t)) + \sum_{m=1}^{2M+1} \Gamma_m q_f(\phi_i(t)-\phi_j(t)+\bar{\omega}\tau_m). \tag{11}$$

By comparing each Fourier coefficient of Eq. (11) up to the $M$th harmonic, we obtain

$$\widetilde{a_k} = \frac{\epsilon_c}{\epsilon_f} a_k^{(c)} + \sum_{m=1}^{2M+1} \Gamma_m a_k^{(f)} e^{ik\bar{\omega}\tau_m}. \tag{12}$$

Although the Fourier coefficients of the harmonics higher than $M$ in $q_c(\psi)$ and $q_f(\psi)$ generally have nonzero values, we can minimize their contributions by taking $M$ sufficiently larger than the number of harmonics in which $q_c(\psi)$ and $q_f(\psi)$ have non-negligible Fourier components. Equation (12) is rewritten in a matrix form as

$$\begin{pmatrix} A_0 \\ A_1 \\ A_2 \\ \vdots \\ A_M \\ B_1 \\ B_2 \\ \vdots \\ B_M \end{pmatrix} = \begin{pmatrix} 1 & 1 & \cdots & 1 \\ \cos(\bar{\omega}\tau_1) & \cos(\bar{\omega}\tau_2) & \cdots & \cos(\bar{\omega}\tau_{2M+1}) \\ \cos(2\bar{\omega}\tau_1) & \cos(2\bar{\omega}\tau_2) & \cdots & \cos(2\bar{\omega}\tau_{2M+1}) \\ \vdots & \vdots & \ddots & \vdots \\ \cos(M\bar{\omega}\tau_1) & \cos(M\bar{\omega}\tau_2) & \cdots & \cos(M\bar{\omega}\tau_{2M+1}) \\ \sin(\bar{\omega}\tau_1) & \sin(\bar{\omega}\tau_2) & \cdots & \sin(\bar{\omega}\tau_{2M+1}) \\ \sin(2\bar{\omega}\tau_1) & \sin(2\bar{\omega}\tau_2) & \cdots & \sin(2\bar{\omega}\tau_{2M+1}) \\ \vdots & \vdots & \ddots & \vdots \\ \sin(M\bar{\omega}\tau_1) & \sin(M\bar{\omega}\tau_2) & \cdots & \sin(M\bar{\omega}\tau_{2M+1}) \end{pmatrix} \begin{pmatrix} \Gamma_1 \\ \Gamma_2 \\ \vdots \\ \vdots \\ \vdots \\ \vdots \\ \Gamma_{2M} \\ \Gamma_{2M+1} \end{pmatrix}, \tag{13}$$

where $A_k = \mathrm{Re}[\{\widetilde{a_k} - (\epsilon_c/\epsilon_f)a_k^{(c)}\}/a_k^{(f)}]$ and $B_k = \mathrm{Im}[\{\widetilde{a_k} - (\epsilon_c/\epsilon_f)a_k^{(c)}\}/a_k^{(f)}]$. Thus, when the values of $\tau_1, \tau_2, \ldots$, and $\tau_{2M+1}$ are determined, the corresponding values of $\Gamma_1, \Gamma_2, \ldots$, and $\Gamma_{2M+1}$ can be derived by solving Eq. (13).

Although there is no specified method of selecting the values of $\tau_1, \tau_2, \ldots$, and $\tau_{2M+1}$, we should select them considering the following two points. First, $\tau_m$ should be selected such that it is comparable to or smaller than $(2\pi/\bar{\omega})^{-1}$, otherwise the validity of the approximation given in Eq. (10) will be lost. Second, $\Sigma_{m=1}^{2M+1}|\Gamma_m|$, which we will hereafter denote as $G$, should not have a large value for the validity of the phase model, the reason for which will be described in Sec. IV.

In order to find the values of $\tau_m$ and $\Gamma_m$ satisfying these requirements, we have selected $\tau_m$'s such that the following relation is satisfied:

$$\tau_m = \frac{2\pi}{\bar{\omega}} \cdot \mathrm{frac}\left(\frac{\alpha m}{2M+1} - \frac{\bar{\omega}\tau_0}{2\pi}\right) + \tau_0, \tag{14}$$

where $\mathrm{frac}[\alpha m/(2M+1) - \bar{\omega}\tau_0/(2\pi)]$ indicates the fractional part of $\alpha m/(2M+1) - \bar{\omega}\tau_0/(2\pi)$, and $\tau_0$ is the time required to process the sum of the outputs from all the oscillators. Then, $\Gamma_1, \Gamma_2, \ldots$, and $\Gamma_{2M+1}$ are calculated from Eq. (13) with changing $\alpha$. Here, it is sufficient to change $\alpha$ within the range of $0 \leqslant \alpha < 2M+1$ because the values of $\tau_m$ do not vary when $\alpha$ is added by multiples of $2M+1$. Thus, $\tau_1, \tau_2, \ldots$, and $\tau_{2M+1}$ are systematically determined only by selecting $\alpha$ such that $G$ does not have a large value. In fact, we can find the appropriate values of $\tau_m$ and hence $\Gamma_m$ rapidly by using this scheme. It is noted that even when this scheme is used, $G$ cannot take a smaller value than the maximum value of $|A_k|$ and $|B_k|$, which can be easily proved from Eq. (13) such that $|A_k| = |\Sigma_{m=1}^{2M+1} \cos(k\bar{\omega}\tau_m)\Gamma_m| \leqslant \Sigma_{m=1}^{2M+1}|\Gamma_m| = G$. Hence, $\tilde{q}(\psi)$ should be determined so that $\mathrm{Max}[|A_k|, |B_k|]$ does not take a large value.

## III. SIMULATION

Now, let us confirm the validity of this method through a simulation. Here, we employ the Bonhoeffer–van der Pol model, which is known as a representative model describing limit-cycle oscillations [18]. We consider a case where the oscillators are coupled to each other by the same coupling strength, and then the model is described as

$$\begin{pmatrix} h\dot{u}_i \\ \dot{v}_i \end{pmatrix} = \begin{pmatrix} -b_i v_i + u_i - u_i^3/3 \\ u_i + cv_i + d \end{pmatrix} + \frac{\epsilon_c}{N}\sum_{j=1}^{N}(u_j(t) - u_i(t))\begin{pmatrix} 1 \\ 0 \end{pmatrix}, \tag{15}$$

where the first term in the right-hand side denotes a set of functions describing a limit cycle, while the second term denotes the coupling between the oscillators. Here, we have assumed that the oscillators are coupled only through the variable $u$ by its difference. The parameters $h$, $c$, and $d$ are set at 0.2, 0, and 0.8, respectively. $b_i$ is set at $b_i=1.0005-0.0001i$, where $i$ is an index, so that the natural periods of the oscillators are slightly distributed. Actually, the natural periods are found to range from 4.51 to 4.54 under these conditions. The natural coupling strength $\epsilon_c$ is set at 0.05, whereas the total number of the oscillators $N$ is set at 100. We assume that $\Sigma_{j=1}^{N}u_j(t)$ is the only observable, and apply the feedback signals as

$$\begin{pmatrix} h\dot{u}_i \\ \dot{v}_i \end{pmatrix} = \begin{pmatrix} -b_i v_i + u_i - u_i^3/3 \\ u_i + cv_i + d \end{pmatrix} + \frac{\epsilon_c}{N}\sum_{j=1}^{N}(u_j(t) - u_i(t))\begin{pmatrix} 1 \\ 0 \end{pmatrix} + \frac{\epsilon_f}{N}\sum_{m=1}^{2M+1}\Gamma_m\sum_{j=1}^{N}u_j(t-\tau_m)\mathbf{r}. \tag{16}$$

The coupling strength under the feedback signals $\epsilon_f$ is set at 0.07, which is sufficiently small so that the phase description is valid, but sufficiently large so that the oscillators can be well synchronized under the feedback. $\mathbf{r}$ is a two-dimensional unit vector and here, the cases of $\mathbf{r}=(1,0)^T$ and $(0,1)^T$ are investigated. In the following simulations, as a target state, we will select a symmetric $n$-cluster state ($n=2$, 3, and 4) [21] in which the population of the oscillators is split into $n$ equally populated clusters with the phase difference between adjacent clusters being $2\pi/n$, or a desynchronized state in which the oscillators are not synchronized and their phases are distributed uniformly [14].

First, the coupling functions $q_c(\psi)$, $q_f(\psi)$, and $\tilde{q}(\psi)$ should be determined. $q_c(\psi)$ is derived by applying the method described in Ref. [20] to the present model, while $q_f(\psi)$ is derived by performing the procedures shown in Appendix with $\tau_0$ set at 0.5. The obtained functional forms of $q_c(\psi)$ and $q_f(\psi)$ for $\mathbf{r}=(1,0)^T$ and $(0,1)^T$, and their absolute values of the Fourier coefficients $|a_k^{(c)}|$ and $|a_k^{(f)}|$ are shown in Fig. 1. We find that $|a_k^{(c)}|$ and $|a_k^{(f)}|$ decrease rapidly as $k$ increases. Hence, we select $M$, the number of the highest harmonic of $\tilde{q}(\psi)$, as 10, so that it is sufficiently larger than the number of harmonics in which $q_c(\psi)$ and $q_f(\psi)$ have nonnegligible Fourier components.

On the other hand, the functional form of $\tilde{q}(\psi)$ is determined using the result of the linear stability analysis of symmetric cluster states reported previously [21]. Namely, $\tilde{q}(\psi)$ is selected such that the real parts of the eigenvalues are all sufficiently negative only for the target state when the target state is a symmetric $n$-cluster state, whereas eigenvalues having non-negative real parts exist for all symmetric cluster states when the target state is a desynchronized state. Here, $\tilde{q}(\psi)$ should be determined carefully so that $\mathrm{Max}[|A_k|,|B_k|]$ does not have a large value, because otherwise, $G$ becomes

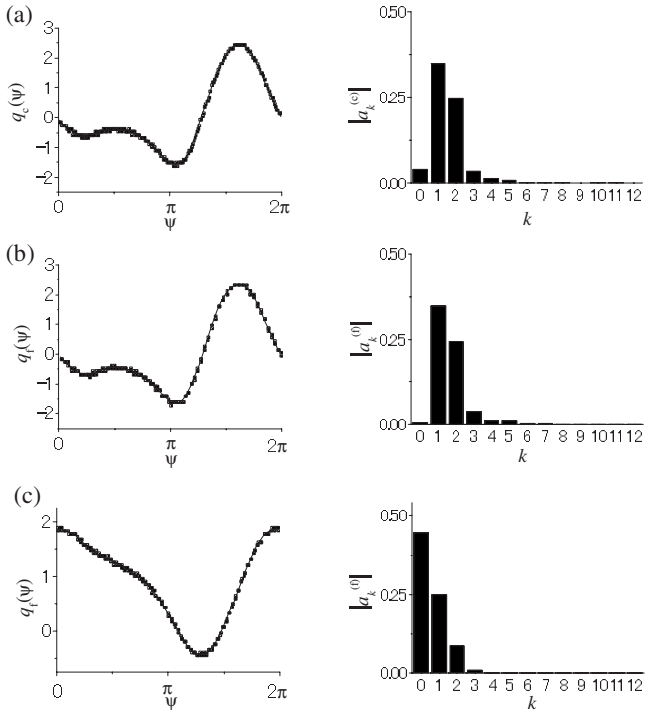


FIG. 1. Functional forms of (a) $q_c(\psi)$, (b) $q_f(\psi)$ for $\mathbf{r}=(1,0)^T$, and (c) $q_f(\psi)$ for $\mathbf{r}=(0,1)^T$ (graphs on the left-hand side). The data are obtained by using the method described in Ref. [20] (black dots), and they are fitted by a function $\gamma_0+\Sigma_{k=1}^{12}(\beta_k\sin(k\psi)+\gamma_k\cos(k\psi))$ with the fitting parameters $\beta_k$ and $\gamma_k$ (solid lines). In the graphs on the right-hand side, the absolute values of the complex Fourier coefficients $|a_k^{(c)}|$ and $|a_k^{(f)}|$ are shown. Note that $|a_k^{(c)}|$ and $|a_k^{(f)}|$ are given as $\sqrt{\beta_k^2+\gamma_k^2}/2$ for $k\geqslant 1$ and $\gamma_0$ for $k=0$.

large. The functional forms of $\tilde{q}(\psi)$ thus obtained for desynchronized, two-cluster, three-cluster, and four-cluster states are shown in Fig. 2.

Next, we will determine the values of $\tau_m$ and $\Gamma_m$, and perform simulations using them. In the simulations, the Runge-Kutta method will be employed with time intervals of 0.02 and with the initial condition of $u_i=v_i=1.5$ for all $i$. First, we show the case where the target state is three-cluster state with $\mathbf{r}=(1,0)^T$. Figure 3 shows the relation between $\alpha$ and $G$. It is found that $G$ varies significantly with $\alpha$ and takes a minimum value 4.08 at $\alpha=1.030$, based on which we derive $\tau_m$ and $\Gamma_m$ using Eqs. (14) and (13), respectively.

Figure 4 shows the temporal evolutions of the relative phases of the oscillators, where the feedback signal is applied during $500\leqslant t\leqslant 1500$. We define the relative phase of the $i$th oscillator $\psi_i$ $(i\geqslant 2)$ as $\psi_i(t_1^{(K)})=2\pi(t_i^{(K')}-t_1^{(K)})/(t_1^{(K+1)}-t_1^{(K)})$, where $t_1^{(K)}$ and $t_i^{(K')}$ denote the time when the first and $i$th oscillators take maximum values of $v$ at the $K$th and $K'$th cycles, respectively, with $K$ and $K'$ satisfying $t_1^{(K)}\leqslant t_i^{(K')}<t_1^{(K+1)}$. It is evident that the oscillators are synchronized with an in-phase before the feedback signal is applied. When the feedback signal is switched on, the phases become distributed transiently, and then gradually divide into three clusters. The phase difference between the adjacent clusters is found to be approximately $2\pi/3$, and the numbers of oscil-

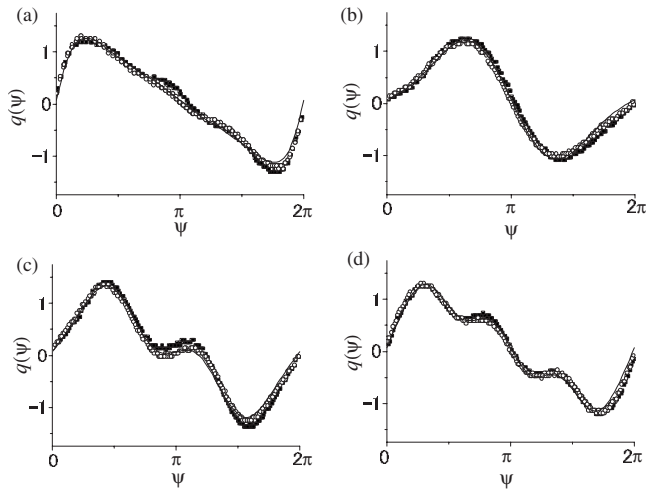


FIG. 2. Functional forms of $\tilde{q}(\psi)$ for (a) desynchronized, (b) two-cluster, (c) three-cluster, and (d) four-cluster states, which are given as $\tilde{q}(\psi)=\sin\psi+0.4\sin 2\psi+0.2\sin 3\psi+0.08\sin 4\psi+0.04\sin 5\psi+0.02\sin 6\psi+0.01\sin 7\psi+0.01\sin 8\psi+0.07$, $\tilde{q}(\psi)=\sin\psi-0.3\sin 2\psi+0.07$, $\tilde{q}(\psi)=\sin\psi+0.3\sin 2\psi-0.2\sin 3\psi+0.07$, and $\tilde{q}(\psi)=\sin\psi+0.3\sin 2\psi+0.2\sin 3\psi-0.1\sin 4\psi+0.07$, respectively (solid lines). Note that $\tilde{a}_k$ and $\tilde{a}_{-k}$ are set at zero when $\tilde{q}(\psi)$ does not have a Fourier component in the $k$th harmonic for $k\leqslant M$, where $M$ is taken as 10. The coupling functions under the feedback in the cases of $\mathbf{r}=(1,0)^T$ (open circles) and $\mathbf{r}=(0,1)^T$ (filled squares) are also shown, which are derived by using the method described in Ref. [20].

lators that belong to the three clusters are 38, 30, and 32. When the feedback signal is switched off, the three clusters converge, which leads to in-phase synchronization again.

Figure 5 shows the temporal evolutions of $u_i$. Here, the data of three oscillators belonging to different clusters are shown separately. It is evident that each oscillator oscillates with an amplitude of ~4, and its waveform does not differ significantly with or without the feedback signal. When the feedback signal is switched on, only the phase relationship changes. Figure 6 shows the magnitude of the feedback signal described as $\epsilon_f N^{-1}\Sigma_{m=1}^{2M+1}\Gamma_m\Sigma_{j=1}^{N}u_j(t-\tau_m)$. We find that the magnitude of the feedback signal is found to be smaller than ~0.3, which is sufficiently smaller than the oscillation amplitude of $u_i$. These results do not contradict the validity of the phase description, where the contribution of the feedback term is sufficiently smaller than that of the term associated with the limit cycle [see Eq. (8)]. On the other hand, the coupling function under the feedback signal, which is derived by using the method described in Ref. [20], is shown in Fig. 2(c) (open circles). It is found that the obtained coupling function is surprisingly in good agreement with $\tilde{q}(\psi)$. Thus, the functional form of the coupling function is actually well-controlled by the feedback.

The cases where $\tau_m$ and $\Gamma_m$ are derived from different values of $\alpha$ are also investigated. Here, $\alpha$ is selected as 1.152, 0.939, and 1.276, so that $G$ takes values of 21.50, 34.84, and 49.92, respectively (see Fig. 3). Figures 7 and 8 show the relative phases and the magnitude of the feedback signal in these cases, respectively. In the cases of $\alpha=1.152$ and $\alpha=0.939$, a three-cluster state is obtained under the feedback, with the magnitude of the feedback signal being even smaller than ~0.3. However, in the case of $\alpha=1.276$, in-phase state is found to appear even under the feedback, although the target state is set at a three-cluster state. In this case, the magnitude of the feedback signal is extremely large so that it is comparable to the oscillation amplitude [Fig. 8(c)], which suggests that the phase description is no longer

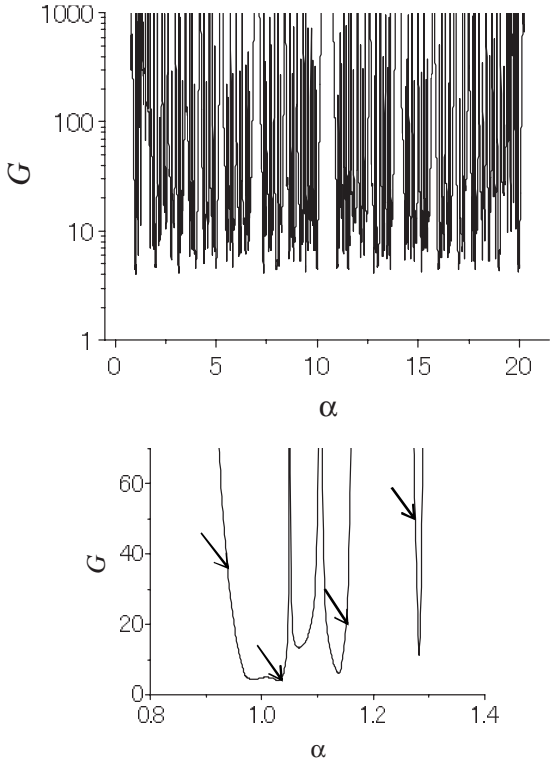


FIG. 3. $\alpha$ dependence of $G$ in the case where the target state is a symmetric three-cluster state and $\mathbf{r}=(1,0)^T$. $\alpha$ is changed from 0 to 21 with a step of 0.001. The lower graph shows a magnified view of the upper graph. Note that $G$ in the upper graph is described in a log scale, whereas that in the lower one is described in a linear scale. The values of $\alpha$ used in the simulations are indicated by arrows.

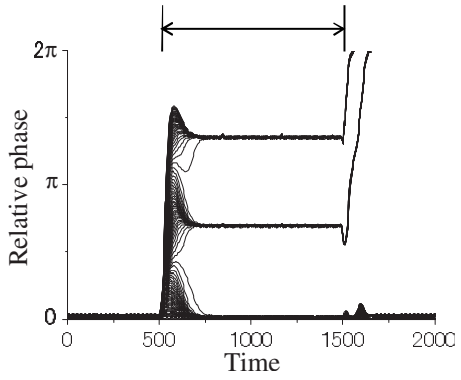


FIG. 4. Temporal evolutions of the relative phases $\psi_i$ with $i=2,3,\ldots,$ and 100 (solid lines) when the target state is a three-cluster state with $\mathbf{r}=(1,0)^T$. $\tau_m$ and $\Gamma_m$ are derived using the value of $\alpha=1.030$. The feedback signal is applied during $500\leqslant t\leqslant 1500$ (left-right arrow).

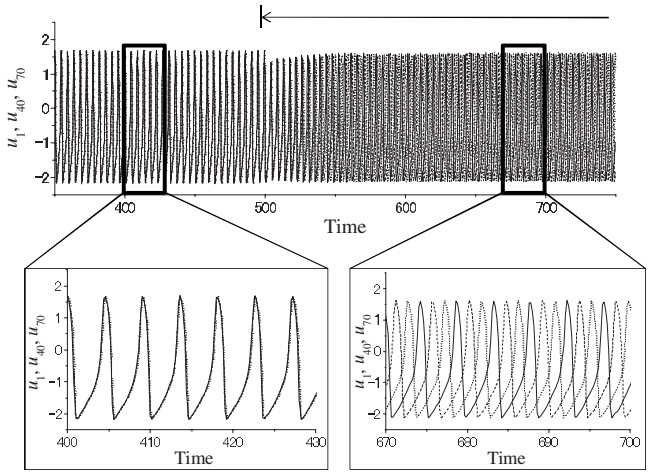


FIG. 5. Temporal evolutions of $u_i$ when the target state is a three-cluster state with $\mathbf{r}=(1,0)^T$. The data of three oscillators belonging to different clusters [$i=1$ (solid line), 40 (dashed line), and 70 (dotted line)] are shown. The feedback signal is applied for $t \geqslant 500$ (arrow). $\tau_m$ and $\Gamma_m$ are derived using the value of $\alpha=1.030$. The left- and right-lower graphs show the magnified views before and after the onset of the feedback signal. Note that the three oscillatory curves are overlapped in the left-lower graph.

valid. Thus, $G$ is an important quantity for the applicability of the present method, and $\alpha$ should be selected such that $G$ does not have a large value.

Next, we show the results when the target state is changed in sequence from desynchronized to two-cluster to three-cluster to four-cluster state. We consider the cases for $\mathbf{r}=(1,0)^T$ and $\mathbf{r}=(0,1)^T$ separately. For each target state, $\tau_m$ and $\Gamma_m$ are derived from the value of $\alpha$ in which $G$ takes its minimum value. Then, $G$ is generally found to be smaller than $\sim 20$, which is at most $\sim 8$ times larger than $\mathrm{Max}[|A_k|,|B_k|]$ (see tables in Fig. 9). The distribution densities of the relative phases in the cases of $\mathbf{r}=(1,0)^T$ and $\mathbf{r}=(0,1)^T$ are shown in Figs. 9(a) and 9(b), respectively. In

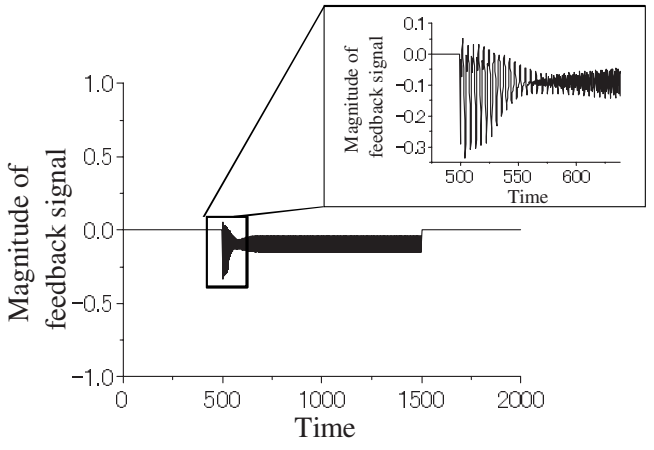


FIG. 6. Temporal evolution of the magnitude of the feedback signal $(\epsilon_f/N)\Sigma_{m=1}^{2M+1}\Gamma_m\Sigma_{j=1}^{N}u_j(t-\tau_m)$ when the target state is a three-cluster state with $\mathbf{r}=(1,0)^T$. $\tau_m$ and $\Gamma_m$ are derived using the value of $\alpha=1.030$. The feedback signal is applied during $500 \leqslant t \leqslant 1500$. The inset shows a magnified view at the onset of the feedback signal.

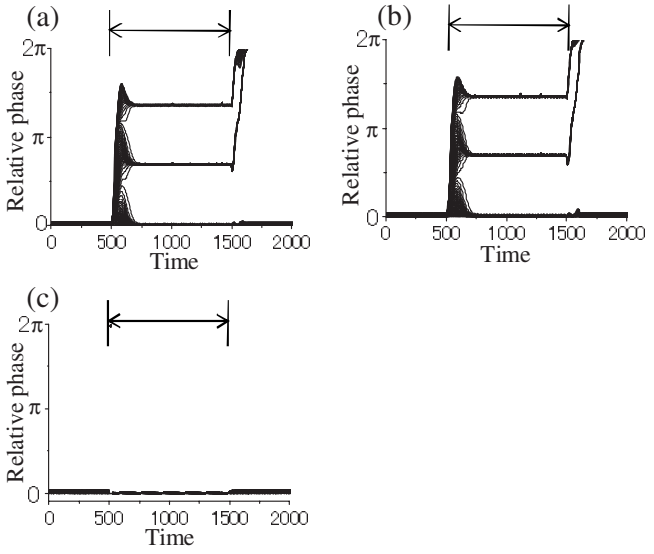


FIG. 7. Temporal evolutions of the relative phases $\psi_i$ with $i=2,3,\ldots,$ and 100 (solid lines), when the target state is a three-cluster state and $\mathbf{r}=(1,0)^T$. The cases of (a) $\alpha=1.152$ ($G=21.50$), (b) $\alpha=0.939$ ($G=34.84$), and (c) $\alpha=1.276$ ($G=49.92$) are shown. The feedback signal is applied during $500 \leqslant t \leqslant 1500$ (left-right arrows).

both cases, the target states are excellently reproduced by the feedback. Furthermore, these behaviors are still obtained even when a finite amount of noise is introduced in the model, as far as it is not too large (data not shown). The coupling functions obtained under the feedback signals are shown in Fig. 2. It is evident that the obtained coupling functions are generally in good agreement with the target coupling function $\tilde{q}(\psi)$. Thus, it is confirmed that various dynamical behaviors are obtainable by controlling coupling functions using the present method.

## IV. DISCUSSION

We have proposed a method to control the dynamics of coupled oscillators by regulating the coupling function through multilinear feedback, and have confirmed its validity through simulations. Although a previously reported study [14,15] suggested that the coupling function is well regulated by nonlinear feedback, it has a problem for practical use in that an individual output from each oscillator has to be measured. On the contrary, in our method, control is possible as far as we can measure the sum of the outputs from all the oscillators. This fact is extremely advantageous because it is often practically difficult to measure individual outputs from all oscillators and to process them rapidly, particularly when the number of oscillators becomes large, e.g., neuronal systems. Thus, the present method will eventually be applied to various systems without practical restrictions.

By using the present method, the coupling function can be controlled up to the $M$th harmonic. Although the harmonics higher than $M$ are not controlled, we can minimize their contribution by taking $M$ larger than the number of harmonics in which $q_c(\psi)$ and $q_f(\psi)$ have nonnegligible Fourier

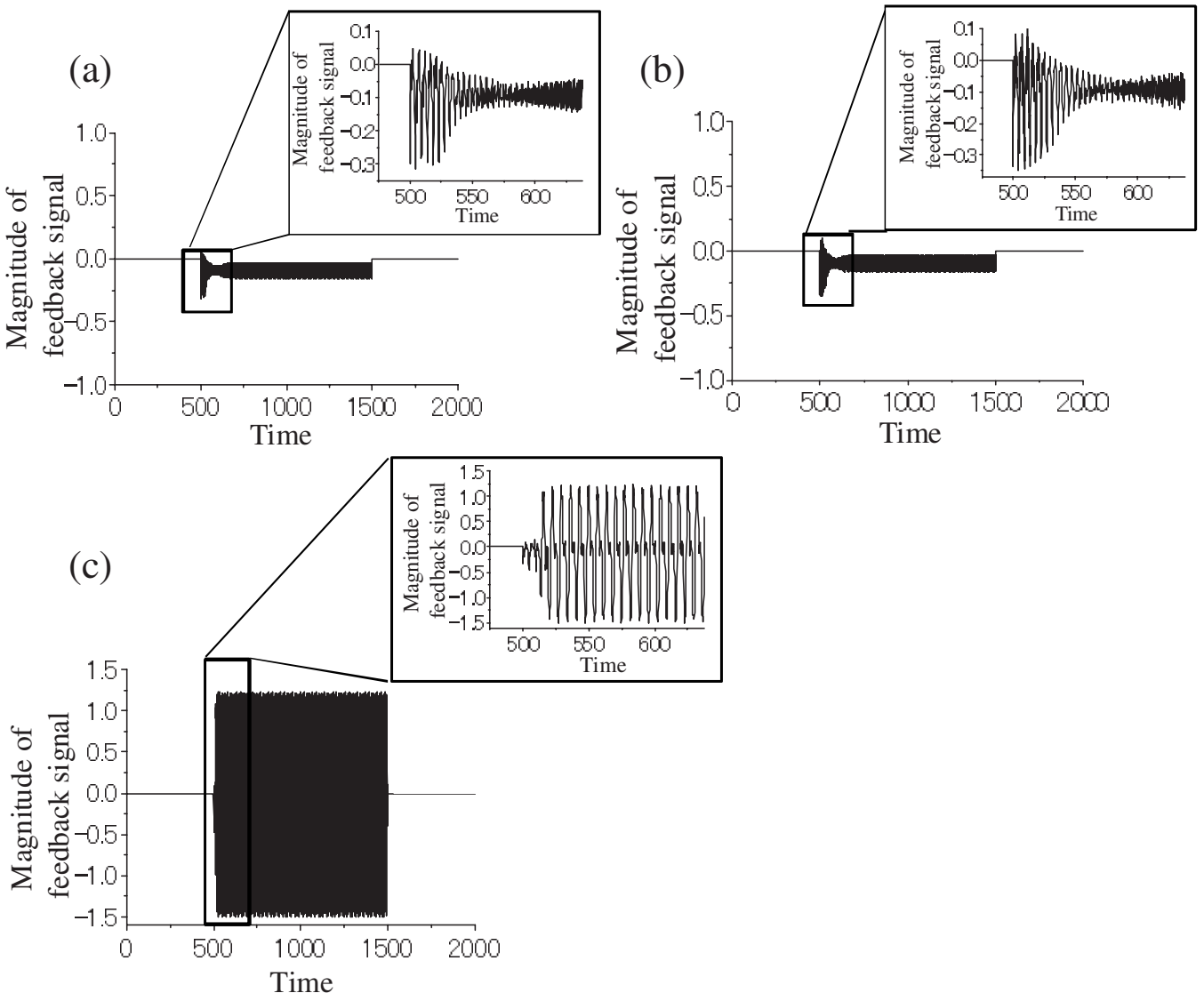


FIG. 8. Temporal evolutions of the magnitude of the feedback signals $(\epsilon_f/N)\Sigma_{m=1}^{2M+1}\Gamma_m\Sigma_{j=1}^{N}u_j(t-\tau_m)$ when the target state is a three-cluster state with $\mathbf{r}=(1,0)^T$. The cases of (a) $\alpha=1.152$ ($G=21.50$), (b) $\alpha=0.939$ ($G=34.84$), and (c) $\alpha=1.276$ ($G=49.92$) are shown. The feedback signal is applied during $500\leqslant t\leqslant 1500$. The insets show magnified views at the onset of the feedback signal.

components. Although the higher harmonics could also be controlled also in the previous study [14,15], this calculation was extremely complex when the number of harmonics became large because of the nonlinearity of the feedback. In contrast, in the present method, it is quite easy to derive $\tau_m$ and $\Gamma_m$ even when $M$ is large. Thus, it is expected that various behaviors that require higher harmonics of coupling function can be easily obtained by employing a large value of $M$ in the present method.

We have shown in the simulation that the control fails for a large value of $G$ [Fig. 7(c)]. The reason why $G$ should not be large is qualitatively explained in the following manner. When we derive Eq. (13), $q_f(\phi_i(t)-\phi_j(t-\tau_m))$ appearing in Eq. (8) is approximated to $q_f(\phi_i(t)-\phi_j(t)+\bar{\omega}\tau_m)$, using Eq. (10). However, when $G$ is extremely large, the discrepancy between $q_f(\phi_i(t)-\phi_j(t-\tau_m))$ and $q_f(\phi_i(t)-\phi_j(t)+\bar{\omega}\tau_m)$ will be amplified by the large $\Gamma_m$'s. Then, the contribution of the feedback term becomes large, and as a consequence, the validity of the phase description given in Eq. (8) is completely lost.

Thus, we need to determine $\tau_m$ and $\Gamma_m$ so that $G$ does not have a large value. In this respect, the present method has an advantage in that we can arbitrarily select $\tau_m$'s so that $G$ does not become large, in contrast to the previous study, where the delays and strengths of the feedback signals were uniquely determined once the target coupling function was determined [14,15]. In fact, by using the present method, we can easily find the parameter sets of $\tau_m$ that can be used to avoid making $G$ so large.

We note that the present method is not applicable when $\mathrm{Max}[|A_k|,|B_k|]$ is large because $G$ cannot have a value smaller than $\mathrm{Max}[|A_k|,|B_k|]$. Nevertheless, it will often be possible to make $\mathrm{Max}[|A_k|,|B_k|]$ small by selecting the vector $\mathbf{r}$ and the observable $\Sigma_{j=1}^{N}p(\mathbf{x}_j)$ properly. Thus, the arbitrary property of $\mathbf{r}$ and $p(\mathbf{x}_j)$ will be beneficial for expanding the applicability of the present method.

(a)

| | (ii) | (iii) | (iv) | (v) |
|---|---|---|---|---|
| $G$ | 5.13 | 3.29 | 4.08 | 4.30 |
| Max[$\|A_k\|$,$\|B_k\|$] | 2.65 | 1.65 | 2.02 | 1.65 |
| $G$/Max[$\|A_k\|$,$\|B_k\|$] | 1.94 | 2.00 | 2.02 | 2.62 |

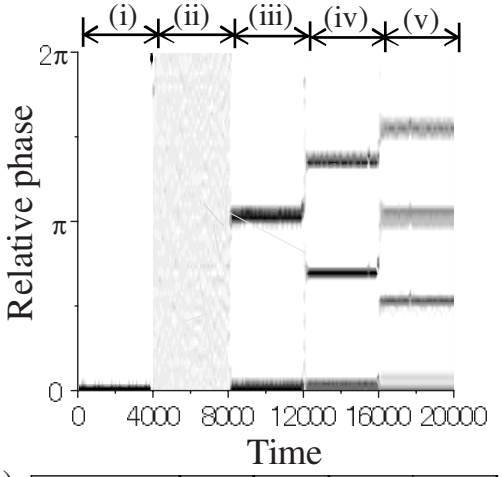


(b)

| | (ii) | (iii) | (iv) | (v) |
|---|---|---|---|---|
| $G$ | 20.11 | 8.36 | 11.64 | 13.09 |
| Max[$\|A_k\|$,$\|B_k\|$] | 5.81 | 2.99 | 2.99 | 1.66 |
| $G$/Max[$\|A_k\|$,$\|B_k\|$] | 3.46 | 2.80 | 3.89 | 7.89 |

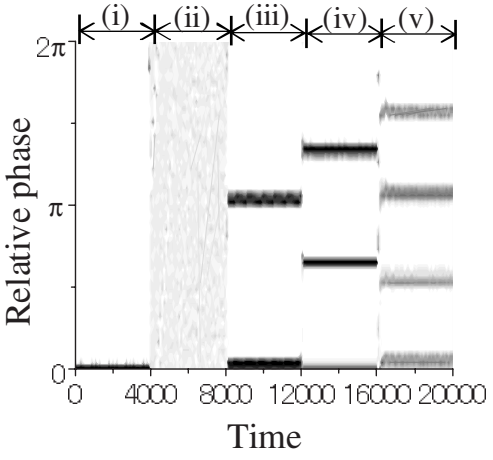


FIG. 9. Temporal evolutions of the distribution density of relative phases in the cases of (a) $\mathbf{r}=(1,0)^T$ and (b) $\mathbf{r}=(0,1)^T$. The distribution density is shown as gray shaded region. The target state is changed in sequence from (ii) desynchronized to (iii) three-cluster to (iv) three-cluster to (v) four-cluster state. In a state (i), the feedback signal is not applied. The values of $G$, Max[$|A_k|$,$|B_k|$], and $G$/Max[$|A_k|$,$|B_k|$] for each target state are listed in tables.

When multiple stable states exist in a system described by Eq. (6), the state obtained through the feedback should depend on initial conditions or noises, and thus, the target state is not necessarily obtained. In fact, we have found that the number of oscillators in each cluster is not completely identical (38, 30, and 32; see Fig. 4), which is due to the presence of stable points for several three-cluster states with different sizes of clusters other than symmetric three-cluster state [3]. Thus, it is desirable, if possible, to set $\tilde{q}(\psi)$ so that stable states other than the target state do not exist, or at least, have small basins of attractions.

In the present method, we have assumed that the oscillators are coupled to each other by the same coupling strength $\epsilon_c$ and that the observable is measured uniformly from all of the oscillators, with the feedback signals uniformly applied to all of the oscillators. However, we expect that the present method can be extended to a system where these assumptions are not necessary. The generalization of the present model is now in progress, which will lead to various practical applications, such as the desynchronization of pathologically synchronized neurons and the stabilization of phase relationships in robots performing cyclic actions.

## APPENDIX: DERIVATION OF $q_f(\psi)$

Consider a couple of oscillators that are separated from the system, and that artificially couple with each other as

$$\dot{\mathbf{x}}_1 = \mathbf{F}_1(\mathbf{x}_1) + \epsilon' p(\mathbf{x}_2(t-\tau_0))\mathbf{r}, \tag{A1}$$

$$\dot{\mathbf{x}}_2 = \mathbf{F}_2(\mathbf{x}_2) + \epsilon' p(\mathbf{x}_1(t-\tau_0))\mathbf{r}, \tag{A2}$$

where $\tau_0$ is here defined as the time required to process the output from an oscillator, which is preferably shorter than the natural oscillation period. The coupling strength $\epsilon'$ is adjusted such that the oscillation periods will be affected by the coupling under the condition that synchronization does not occur. When the period of one of the oscillators is obtained as a function of the phase difference $\psi_{12} \equiv \phi_1(t) - \phi_2(t)$, we can derive the coupling function under this artificial interaction $\hat{q}(\psi_{12})$ up to the first order of $\Delta T_1$ as [20]

$$\hat{q}(\psi_{12}) \approx -\frac{2\pi\Delta T_1(\psi_{12})}{\epsilon' T_1^2}, \tag{A3}$$

where $T_1$ is the natural period of the first oscillator and $\Delta T_1(\psi_{12})$ is the deviation from it when the phase difference is $\psi_{12}$. On the other hand, by considering the phase-reduction process of Eq. (A1), $\hat{q}(\psi_{12})$ is found to be described as

$$\hat{q}(\psi_{12}) = \frac{1}{2\pi}\int_0^{2\pi} d\theta \mathbf{Z}(\phi_1(t)+\theta)\cdot p(\mathbf{x}_0(\phi_2(t-\tau_0)+\theta))\mathbf{r}. \tag{A4}$$

Then, by comparing Eq. (A4) with Eq. (9) for an individual coupling between two oscillators, we find

$$\hat{q}(\psi_{12}) = q_f(\phi_1(t) - \phi_2(t-\tau_0)) \approx q_f(\psi_{12} + \bar{\omega}\tau_0). \tag{A5}$$

Here, we have used the approximation $\phi_j(t-\tau_0) \approx \phi_j(t) - \bar{\omega}\tau_0$ because $\phi_j$ is nearly equal to $\bar{\omega}$. From Eqs. (A3) and (A5), we obtain

$$q_f(\psi_{12}) \approx -\frac{2\pi\Delta T_1(\psi_{12} - \bar{\omega}\tau_0)}{\epsilon' T_1^2}. \tag{A6}$$

[1] Y. Kuramoto, *Chemical Oscillations, Waves, and Turbulence* (Springer-Verlag, Berlin, 1984).
[2] A. Pikovsky, M. Rosenblum, and J. Kurths, *Synchronization: A Universal Concept in Nonlinear Sciences* (Cambridge University Press, Cambridge, England, 2001).
[3] S. C. Manrubia, A. S. Mikhailov, and D. H. Zanette, *Emergence of Dynamical order: Synchronization Phenomena in Complex Systems* (World Scientific, Singapore, 2004).
[4] J. Buck and E. Buck, Nature (London) **211**, 562 (1966).
[5] E. Klavins and D. E. Koditschek, Int. J. Robot. Res. **21**, 257 (2002).
[6] A. Calvitti and R. D. Beer, Biol. Cybern. **82**, 197 (2000).
[7] R. D. Beer, R. D. Quinn, H. J. Chiel, and R. E. Ritzmann, Commun. ACM **40**, 30 (1997).
[8] E. Marder and R. Calabrese, Physiol. Rev. **76**, 687 (1996).
[9] P. A. Tass, *Phase Resetting in Medicine and Biology: Stochastic Modelling and Data Analysis* (Springer-Verlag, Berlin, 1999).
[10] C. Hauptmann, O. Popovych, and P. A. Tass, Neurocomputing **65**, 759 (2005); Biol. Cybern. **93**, 463 (2005); C. Hauptmann, O. Omel'chenko, O. V. Popovych, Y. Maistrenko, and P. A. Tass, Phys. Rev. E **76**, 066209 (2007).
[11] O. V. Popovych, C. Hauptmann, and P. A. Tass, Phys. Rev. Lett. **94**, 164102 (2005); Biol. Cybern. **95**, 69 (2006).
[12] K. Pyragas, O. V. Popovych, and P. A. Tass, Europhys. Lett. **80**, 40002 (2007).
[13] M. Rosenblum and A. Pikovsky, Phys. Rev. E **70**, 041904 (2004); Phys. Rev. Lett. **92**, 114102 (2004).
[14] I. Z. Kiss, C. G. Rusin, H. Kori, and J. L. Hudson, Science **316**, 1886 (2007).
[15] H. Kori, C. G. Rusin, I. Z. Kiss, and J. L. Hudson, Chaos **18**, 026111 (2008).
[16] E. M. Izhikevich, Neural Comput. **18**, 245 (2006).
[17] D. Hansel, G. Mato, and C. Meunier, Phys. Rev. E **48**, 3470 (1993).
[18] P. S. Landa, *Nonlinear Oscillations and Waves in Dynamical Systems* (Kluwer Academic, Dordrecht, 1996).
[19] I. Z. Kiss, Y. Zhai, and J. L. Hudson, Phys. Rev. Lett. **94**, 248301 (2005).
[20] J. Miyazaki and S. Kinoshita, Phys. Rev. Lett. **96**, 194101 (2006); Phys. Rev. E **74**, 056209 (2006).
[21] K. Okuda, Physica D **63**, 424 (1993).